Accepted Manuscript

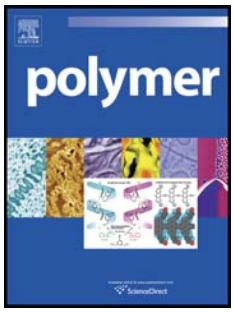

Brittle-Ductile Transition of Double Network Hydrogels: Mechanical Balance of Two Networks as the Key Factor

Saika Ahmed, Tasuku Nakajima, Takayuki Kurokawa, Md. Anamul Haque, Jian Ping Gong

PII: S0032-3861(13)01185-3

DOI: 10.1016/j.polymer.2013.12.066

Reference: JPOL 16704

To appear in: *Polymer*

Received Date: 15 November 2013

Revised Date: 27 December 2013

Accepted Date: 28 December 2013

Please cite this article as: Ahmed S, Nakajima T, Kurokawa T, Haque MA, Gong JP, Brittle-Ductile Transition of Double Network Hydrogels: Mechanical Balance of Two Networks as the Key Factor, *Polymer* (2014), doi: 10.1016/j.polymer.2013.12.066.

Graphical abstract

Brittle-Ductile Transition of Double Network Hydrogels: Mechanical Balance of Two Networks as the Key Factor

Saika Ahmed, Tasuku Nakajima, Takayuki Kurokawa, Md. Anamul Haque, and Jian Ping Gong

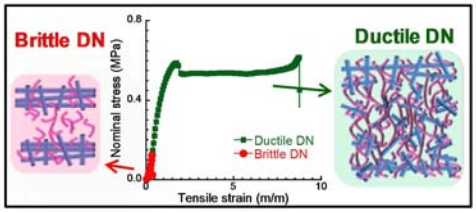

Brittle-Ductile Transition of Double Network Hydrogels: Mechanical Balance of Two Networks as the Key Factor

Saika Ahmed[a], *Tasuku Nakajima*[b], *Takayuki Kurokawa*[b], *Md. Anamul Haque*[b,#] *and Jian Ping Gong*[b,*]

[a]Graduate School of Life Science, Hokkaido University, Sapporo 060-0810, Japan

[b]Faculty of Advanced Life Science, Hokkaido University, Sapporo 060-0810, Japan

[#]Present address: Department of Chemistry, University of Dhaka, Dhaka-1000, Bangladesh

* Corresponding author

Tel. & Fax: +81-11-706-2774, E-mail: gong@mail.sci.hokudai.ac.jp

Key words: Double network hydrogels, fracture, toughness, polymer strand density, mechanical force balance

Abstract

Tough double network (DN) hydrogels are a kind of interpenetrating network (IPN) gels with a contrasting structure; it consists of a rigid and brittle 1st network with dilute, densely cross-linked short chains and a soft and ductile 2nd network with concentrated, loosely cross-linked long chains. In this work, we focus on how the brittle gel changes into a tough one by increasing the amount of ductile component. By comparing the molecular structures of the individual first network and second network gels, we found that the true key mechanical factor that governs the brittle-ductile transition is the fracture stress ratio of the two networks, $\sigma_{f,2}/\sigma_{f,1}$. This ratio is related to the density ratio of elastically effective polymer strands of the two networks, $\nu_{e,2}/\nu_{e,1}$, where the inter-network topological entanglement makes dominant contribution to $\nu_{e,2}$. When $\nu_{e,2}/\nu_{e,1} < k$ =3.8-9.5, the second network fractures right after the fracture of the first network, and the gels are brittle. When $\nu_{e,2}/\nu_{e,1} > k$, only the first network fractures. As a result, the brittle first network serves as sacrificial bonds, imparting toughness of DN gels. The study also confirms that the load transfer between the two networks is via inter-network topological entanglement. This result provides essential information to design tough materials based on the double network concept.

I. Introduction

Double network hydrogels or, DN gels, are regarded as one of the most robust synthetic hydrogels.[1] The tough DN gels have a very special interpenetrating network (IPN) structure. They are comprised of a rigid and brittle 1st network of densely-cross-linked short chains in dilute concentration, and a soft, stretchable 2nd network of loosely-cross-linked long chains in high concentration. The soft second network is densely packed and interpenetrated in the cage of the first network's rigid skeleton, as illustrated in **Scheme 1**. This special contrasting structure makes the DN gels extra-ordinarily tough, significantly different from conventional IPN gels. The typical tough DN gels, referred to as PAMPS/PAAm DN gels, are synthesized using poly(2-acrylamido-2-methylpropane-sulfonic acid) (PAMPS) as the first network and polyacrylamide (PAAm) as the second network.[1] The PAMPS/PAAm DN gels show high extensibility (~2,000% of original length),[1] strength (tensile fracture stress ~5 MPa)[2] and toughness (fracture energy ~1,000 J/m^2).[3,4] Later, many studies have shown that the DN concept is universal and is applicable to various species of polymeric materials, whenever the above

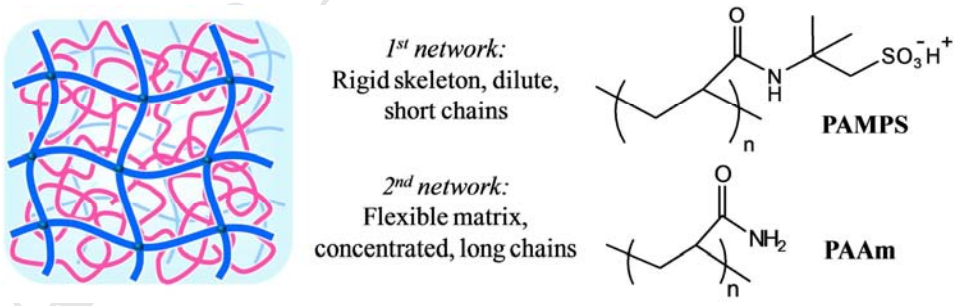

Scheme 1: Illustration of super-tough double network (DN) gels with a contrasting structure. The blue and pink lines represent the 1st and 2nd networks respectively and the filled circles indicate chemical cross-linking points. The two networks do not have internetwork chemical bond, creating a truly interpenetrating network (IPN) structure. The chemical structures of PAMPS and PAAm as first and second networks, respectively, is shown on the right.

mentioned contrasting DN structure is formed.[5-9]

Many experimental and theoretical studies have been performed to reveal the toughening mechanism of the DN gels.[10-14] These studies have revealed that the high toughness of DN gels derives from the internal fracture of the brittle network during deformation, which is observed by yielding, necking, and irreversible softening (the Mullins effect) phenomena upon tensile deformation. The internal fracture of the brittle network delocalizes the stress at the crack tip and dissipates a large amount of energy, which substantially retards the crack growth and therefore toughens the material. Previous studies[1,15] have shown that the structural essence of the tough DN gels can be summarized as follows: 1) Short first network strands and long second network strands, i.e., $N_2>>N_1$, and 2) Low first network concentration and high second network concentration, i.e., $c_2>>c_1$. Here N stands for the number of repeated monomeric units of polymer strands between two *chemically* cross-linked points and c indicates the molar concentration of the monomeric units of polymers.

In this study, we take notice on the latter toughening condition $c_2>>c_1$. The sole first network is very brittle, and the DN gels containing large amount of the second network is ductile and tough. Then, how does the brittle gel change into a ductile and tough one by increasing the amount of the second ductile component c_2? In this paper, we keep the first criteria $N_2/N_1 >> 1$ satisfied and investigate the effect of the two network concentrations c_1 and c_2 on the mechanical behavior of the DN gels. For this purpose, we synthesized 3 sets of DN gels. For each set, we use a constant 1st network cross-linker density but various 2nd network concentrations. First, we prepared PAMPS single network gels with 3 different cross-linker densities. As the swelling degree of a polyelectrolyte hydrogel substantially changes with its cross-linker density, this permits us to modulate c_1 (which is roughly inverse to N_1) only by changing the cross-linker

density for preparing the 1st network. In each set of the PAMPS samples, we synthesized the second network from different AAm monomer concentration, c_{AAm} while keeping the chemical cross-linker density of the second network constant at a very small value. This permits us to keep N_2 as a large constant value, and modulate the concentration of the second network, c_2 near the transition regions. We characterized the strength and toughness of these DN gels and determined the brittle-ductile transition points against c_2. To characterize the internal fracture of these samples, we also carried out the cyclic tensile test. By comparing the tensile behavior of individual single network gels, we found that the brittle-ductile transition is strongly related to the polymer strand density ratio of the two networks, $\nu_{\mathrm{e},2}/\nu_{\mathrm{e},1}$, which indicates that the force balance between the two networks acts as the key structural parameter for this transition.

II. Experimental Section

1. Gel Synthesis

A. Materials. 2-Acrylamido-2-methylpropanesulfonic acid (AMPS) (Toa Gosei Co., Ltd.) was used as received. Acrylamide (AAm) (Junsei Chemical Co., Ltd.) was purified by recrystallizing from chloroform. Both the cross-linker *N,N'*-methylenebis(acrylamide) (MBAA) (Wako Pure Chemical Industries Ltd.) and the initiator 2-oxoglutaric acid (Wako Pure Chemical Industries Ltd.) were used as received.

B. Preparation of t-DN Gel. The first network PAMPS concentration, c_1, was varied by changing the first network cross-linker density c_{1_MBAA} and the second network concentration c_2, by changing the monomer concentration c_{AAm}. Three sets of samples were synthesized. Each set

contains the same c_{1_MBAA} but different c_{AAm}. For simplicity, we coded these DN gels as DN (*x*/*y*); where '*x*' and '*y*' are c_{1_MBAA} (mol%, with respect to the monomer concentration) and c_{AAm} (M), respectively. As has already been clarified in our previous works, conventional DN gels contain some internetwork bonds between the first and second networks, which are formed by copolymerization of the second network with the first network through un-reacted residual double bonds of its cross-linker.[4,16] Since truly independent DN gels (labeled *t*-DN gels) that do not contain any covalent bonds between the two networks have simpler structures than conventional DN gels, in this study we prepared *t*-DN gels for analyzing the properties of the DN gels. The *t*-DN gel samples were prepared using two-step sequential polymerization method with a large amount of initiator in the first network polymerization.[4] First, a glass mold was prepared by sandwiching a silicone rubber spacer (thickness varying from 1~3 mm for different experiments) between two similar glass plates. The 1st network precursor solution was prepared by dissolving 1 M of AMPS, 2, 3, 4 or 6 mol% of MBAA as cross-linker and 1 mol% of 2-oxoglutaric acid as photo-initiator (the molar percentages are respective to the monomer concentration). The solution was then moved to an argon blanket, made oxygen-free by shaking and then poured into the pre-made glass molds. After irradiation with UV light of 365 nm wavelength from both sides for 9 hours in an argon atmosphere, the 1st network gel (PAMPS gel) was obtained. Here, the initiator concentration used was much higher than that used in the conventional DN gels which should inactivate the un-reacted residual cross-linkers of the first network. Next, these PAMPS gels were immersed and swollen in the 2nd network precursor solution which contained 0.9~2 M of AAm, 0.02 mol% of MBAA, and 0.01 mol% of 2-oxoglutaric acid for 3 days. The thickness of the as-prepared PAMPS gels was fixed at 1mm and thicknesses of the swollen PAMPS samples in AAm solutions are the same with those in

pure water and they are tabulated in **Table S1 (Supporting information)**. The swollen PAMPS gels containing AAm monomers were then sandwiched by two glass plates, wrapped, moved to an argon blanket and again irradiated by 365 nm UV light from one side for 10 hours. In this way, the 2nd network was subsequently polymerized in the presence of the 1st network and the interpenetrating double network (DN) gels were obtained. The as-prepared DN gels were then swollen in Milli-Q water for 4-5 days to remove any un-reacted monomer and then used for further tests. The sample codes and compositions used in this work are summarized in **Table 1**. The final thickness of these DN gels after swelling and the subsequent true concentrations of two networks in the DN gels along with the calculation method are shown in the supporting information section **(Supporting Figure S1)**.

For photo-polymerization purpose, we used UV lamps with an intensity of ~4 mW/cm^2 and the distance of the lamps from the sample were maintained as ~10 cm.

C. Preparation of Single Network Gels: Single network PAMPS and PAAm gels were prepared separately from the same precursor solutions of AMPS (1 M AMPS, 2, 3, 4, 6 mol% of cross-linker and 1 mol% of initiator) and AAm (0.8~2 M AAm, 0.02 mol% cross-linker and 0.01 mol% of initiator) respectively as that for synthesizing DN gels.

Table 1. Sample codes and formulations of samples used in this study.

Sample code	**1st network**			**2nd network**		
	[Monomer], c_{AMPS} (M)	[Cross-linker], c_{1_MBAA} (mol%)	[Initiator] (mol%)	[Monomer], c_{AAm} (M)	[Cross-linker], c_{2_MBAA} (mol%)	[Initiator] (mol%)
DN (*x*/*y*)	1	2,3,4,6 (= ***x***)	1	0.8~2(= ***y***)	0.02	0.01
PAMPS	1	2,3,4,6	1	-	-	-
PAAm	-	-	-	0.8~2	0.02	0.01

*All the concentrations mentioned are the in-feed concentrations used in the precursor solutions.
** The cross-linker and initiator concentrations indicate their in-feed concentrations in mol%, with respect to the corresponding monomer concentration.

2. Characterization

A. Tensile Test. Equilibrium swollen samples (in water) were used for tensile tests of DN gels whereas as-prepared samples were used for sole PAAm gels. For sole PAMPS gels, both swollen and as-prepared ones were used. All the tensile tests were carried out at 25°C in air environment and pre-cut dumbbell shaped gel samples (**Figure 1a**) standardized as the JIS-K6251-7 size (length of the thinner portion, *L*: 12mm, width of the thinner portion, *b*: 2mm, thickness, *w*: 1.5~3 mm) were used. A commercial tensile tester Instron 5965 (Instron Co.) equipped with an advanced video extensometer (AVE) was applied for measuring tensile stress-strain (SS) curves of the samples at a fixed tensile velocity of 100 mm/min. For DN gels and PAMPS gels, the accurate strain was measured by real-time observation of the distance

between two white spots marked on the thin portion of the sample with the video extensometer. Only nominal strain was determined in the case of sole PAAm gels, as their high stretchability

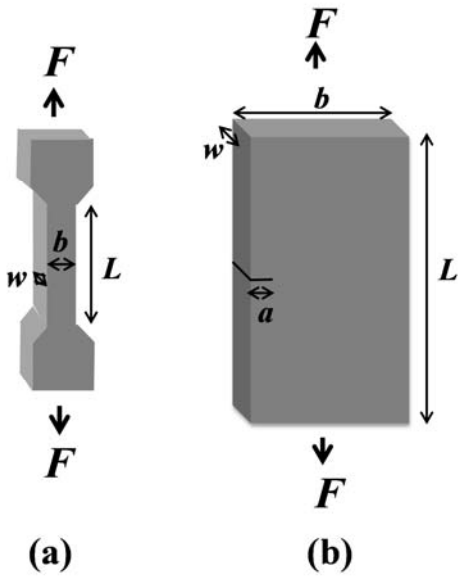

Figure 1: Illustration of different shapes of gel samples used for the characterization: **(a)** dumbbell-shaped sample for tensile/cyclic tensile test and **(b)** bar-shaped sample with a pre-notch for tearing test.

exceeded the view range of the video extensometer. The fracture stress, σ_f (Pa), was obtained from the nominal stress value at the fracture point. The work of extension to fracture, W_{ext} (J/m^3), which is an indication of toughness of materials, was measured from the area under the SS curve until fracture point. The Young's modulus, E, was determined as the slope of nominal stress-strain curves between the strain range of 0.02~0.2. The yield strain and stress, ε_y and σ_y, were determined as the strain and nominal stress at the zero-slope point of the stress-strain curves respectively. Each data was the average of 4 measurements, and the error bars were obtained from their standard deviations.

B. Tensile Test with Pre-notched Samples. In most of our previous studies, tearing test of a trouser-shaped DN sample with pre-crack[17,18] has been used to characterize the gel toughness.[3,19] However, we could not apply this method here for the brittle DN gels because they undergo fracture at the bending point of samples due to their brittle nature. Therefore, in this study, we characterize the gel toughness by performing tensile test on pre-notched bar-shaped DN gel samples at equilibrium swollen state (illustration in **Figure 1b**, length, L= 30 mm, width, b= 10 mm, thickness, w= 4~5 mm, initial notch length, a= 1.5 mm) with the tensile tester Instron 5965 (Instron Co.) at 25°C in the air. One end of the bar-shaped sample was fixed with clamp and the other end was pulled at a constant velocity of 100 mm/min. Crack propagation in mode I (tensile mode of crack opening) was observed as a result of applying force F. For linear elastic samples at small deformation, the stress intensity factor, K_I, ahead of the crack tip is calculated from the following equation,[20]

$$K_I = \sigma\sqrt{a}(1.99 - 0.41x + 18.7x^2 - 38.5x^3 + 53.9x^4) \qquad (1)$$

where, σ is the stress applied ($\sigma=F/w(b-a)$), x is the ratio a/b. The tearing energy, T (J/m^2), defined as the energy required to fracture a unit surface area in the sample, is calculated as,

$$T = K_{Ic}^2(1 - v^2)/E \qquad (2)$$

where, K_{Ic} is the critical stress intensity factor for crack propagation, and it is measured from the critical stress at which the pre-notched crack started to propagate, E is the Young's modulus and v is the Poisson's ratio of the material. We calculated T from Eqs. (1) and (2), using v =0.5 as the gels are incompressible. Strictly speaking, Eqs. (1) and (2) may not be applicable to

non-linear elastic hydrogels. The *T* thus determined might be different by a pre-factor for the non-linear elastic DN gels. We have confirmed that *T* of the ductile DN gels determined by Eqs. (1) and (2) are in agreement with those measured from the tearing test using conventional trouser-shaped samples. So the value of the pre-factor is approximately one for the samples studied.

The fracture energy *T* thus defitermined is two times of the energy required to create a unit fractured surface.[20] Each data was the average of 4 measurements, and the error bars indicate standard deviations.

C. Cyclic Tensile Test. For cyclic tensile test, dumbbell shaped samples standardized as JIS-K6251-7 size, same as those for tensile test **(Figure 1a)**, were used and Instron 5965 (Instron Co.) tensile tester equipped with AVE was applied to record the successive cyclic tensile stress-strain curves. All the cyclic tests were carried out with equilibrium swollen DN gels in the air environment at 25°C. First, the sample was loaded up to a pre-assigned strain, ε_{max} and then unloaded until reaching at a strain zero. Then, they were immediately loaded again up to a pre-fixed higher strain and then unloaded. In this way, the same sample was loaded and unloaded up to gradually increasing strain values until fracture. As in the case of DN gels, a successive loading curve completely overlaps with the unloading curve of the previous cycle,[21,22] we consider only the loading curves instead of the unloading curves for simplicity. The dissipated energy, $U_{hys}(\varepsilon_{max})$ (J/m^3), defined as the area enclosed by the first and second loading curves up to the strain ε_{max} of the first loading, was calculated as

$$U_{\text{hys}}(\varepsilon_{\max}) = \int_0^{\varepsilon_{\max}} \sigma_1 \, d\varepsilon - \int_0^{\varepsilon_{\max}} \sigma_2 \, d\varepsilon \qquad (3)$$

where, σ_1 and σ_2 are the nominal stress values for the first and second loading curves, respectively.

III. Results & Discussion

Tensile Behavior of the DN Gels. The tensile stress-strain (SS) curves of DN (2/*y*), DN (4/*y*) and DN (6/*y*) gels are shown in **Figure 2(a-c)**, respectively. When the 2nd network monomer

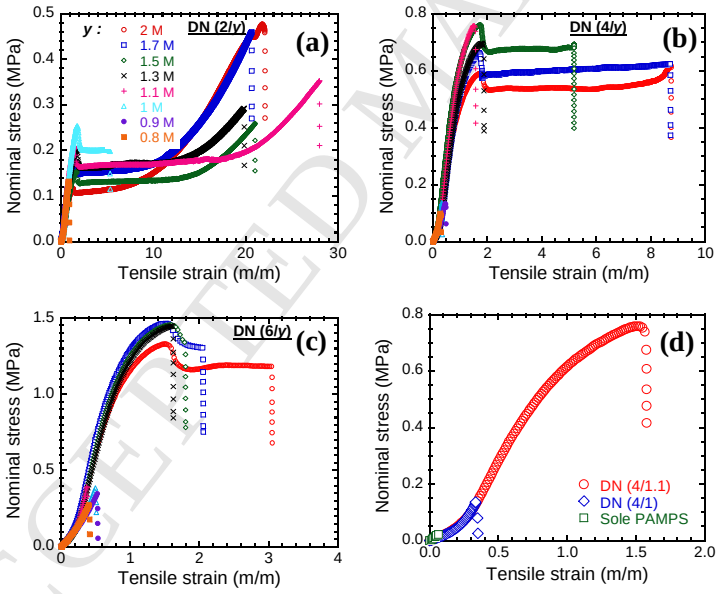

Figure 2: The tensile stress-strain curves of **(a)** DN (2/*y*); **(b)** DN (4/*y*); **(c)** DN (6/*y*) gels and **(d)** sole PAMPS, DN (4/1) and DN (4/1.1) gels, where '*y*' is the AAm monomer concentration in feed. The symbols and colors for different compositions in (b), (c) are the same as in (a). Tensile stretching rate was 100 mm/min. Compared to the brittle ones, the other compositions show much higher toughness.

concentration, *y* is enough high, the DN gels show high fracture stress and fracture strain, and also, the significant 'yielding' phenomenon, which greatly contributes to the excellent toughness of DN gels.[10-13] These robust DN gels which show this exclusive yielding phenomenon are defined as '*ductile*' DN gels. On the other hand, when *y* is reduced while keeping the same 1st network, the fracture stress and strain of the DN gels suddenly decreases after certain points. For example, in the case of DN (4/*y*), fracture stress remarkably decreases when *y* is slightly decreased from 1.1 to 1. Such DN gels undergo fracture much earlier before yielding appears. Thus, these weak DN gels which do not show yield point are defined as '*brittle*' DN gels, and such sudden transformation in fracture parameters has been termed here as '*brittle-ductile transition*'.

When we compared the tensile SS curves of DN (4/1) (brittle) and DN (4/1.1) (ductile) gels with the sole PAMPS gel (**Figure 2d**), it is clearly seen from the fracture point that brittle DN gel is only slightly stronger than the sole PAMPS gel which is extremely brittle. The critical *y* for obtaining ductile DN gels y_c were determined as 1.0, 1.1, and 1.3 M for DN (2/*y*), (4/*y*), and (6/*y*) gels, respectively. We find that as *x* (1st network cross-linker concentration) increases, which correspond to an increase of PAMPS concentration, y_c also increases. This phenomenon suggests that the brittle-ductile transition is not only governed by one network, rather it is governed by the two networks.

Figure 3 shows the Young's modulus (E), fracture stress (σ_f), fracture strain (ε_f), and work of extension (W_{ext}) against the AAm in feed concentration, *y* (**Figure 3**). For a constant set of the PAMPS network, the moduli of the DN gels change very slightly with changing *y* (**Figure 3a**). It means that the brittle-ductile transition does not affect the moduli of DN gels. On the other hand,

the other parameters were remarkably changed in response to brittle-ductile transition. In terms of the fracture stress, the brittle to ductile transition becomes more abrupt for the sample with high cross-linker density of PAMPS (DN (6/*y*)) (**Figure 3b**). In contrast, in terms of fracture strain, we observed an opposite trend (**Figure 3c**). As a result, the work of extension shows an abrupt transition with *y* for all the 3 sets of samples (**Figure 3d**).

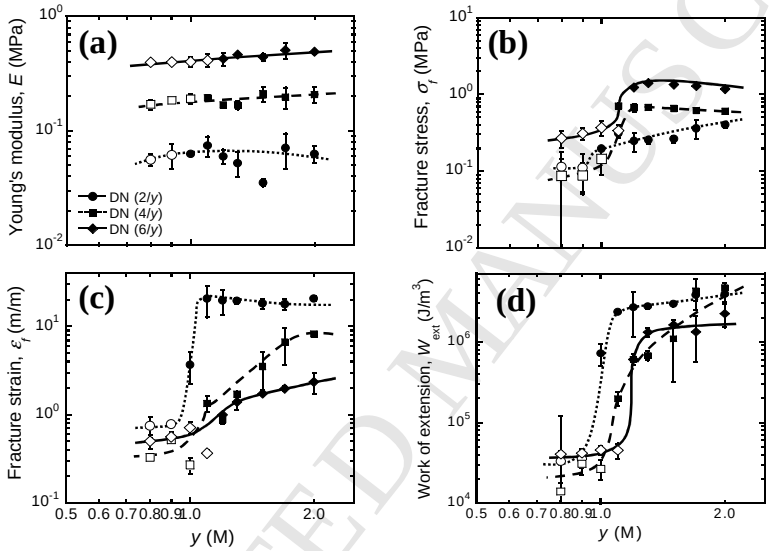

Figure 3: The mechanical toughness characterizing parameters **(a)** Young's modulus, E **(b)** fracture stress, σ_f **(c)** fracture strain, ε_f, and **(d)** work of extension, W_{ext} against AAm monomer concentration in feed, y in DN (2/y), DN (4/y) and DN (6/y) gels. The closed and open symbols indicate ductile and brittle samples respectively and the symbols in (b)-(d) are the same as in (a). In both cases, brittle samples show much smaller values of the parameters showing very low toughness.

Tensile Behavior of Pre-notched DN Gel Samples. To characterize the toughness, we used uniaxial stretching to pre-notched bar-shaped DN gel samples.[23] We calculated the tearing energy of both ductile and brittle DN gel samples by estimating the critical stress intensity factor

for crack propagation (K_{Ic}).[24,25] **Figure 4a** represents the resulting force vs. extension curves for brittle DN (4/0.8), (4/1) and several ductile DN gel samples. It is obvious from this figure that the applied force at which the pre-notch is converted to a running crack is high in all the ductile DN samples; those are, DN (4/1.1), (4/1.5) and (4/2) compositions; but has a much lower value in the case of the brittle compositions DN (4/0.8) and (4/1). That means, a much smaller force is required to initiate crack propagation in the brittle DN gel sample, in contrast to the ductile ones.

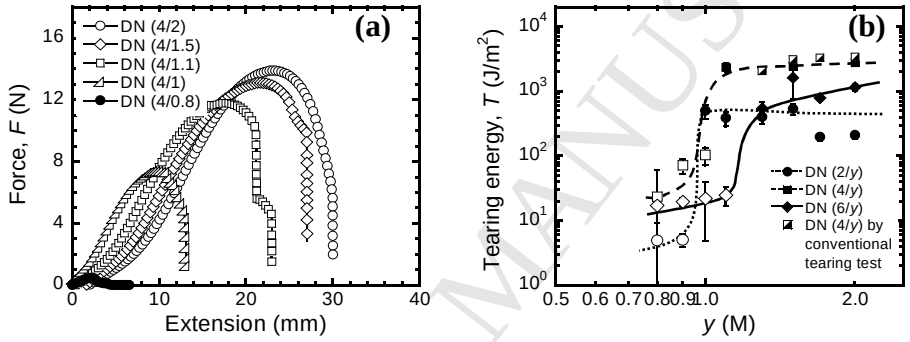

Figure 4: (a) The typical load vs. extension curves for brittle DN (4/0.8), (4/1) and ductile DN (4/1.1), (4/1.5) and (4/2) gels and **(b)** calculated tearing energy, *T* values for DN (2/*y*), (4/*y*) and (6/*y*) gels from tearing test. The brittle DN gels (open symbols in (b)) require much reduced force and energy for crack propagation indicating low crack propagation resistance and hence, very small toughness.

The tearing energy (*T*) calculated using Eq. 1 and Eq. 2 for different brittle and ductile compositions is shown in **Figure 4b**. The *T* measured using conventional trouser-shaped samples for DN (4/*y*) gels are also shown in **Figure 4b** for comparison, and they show a good agreement. An abrupt increase in the tearing energy *T* is observed at critical y_c values, in consistence with the tensile results in **Figure 3d**.

From the above results, we can construct a mechanical phase diagram in the space of concentrations of the first and second networks (**Figure 5**). As the entanglement between the two

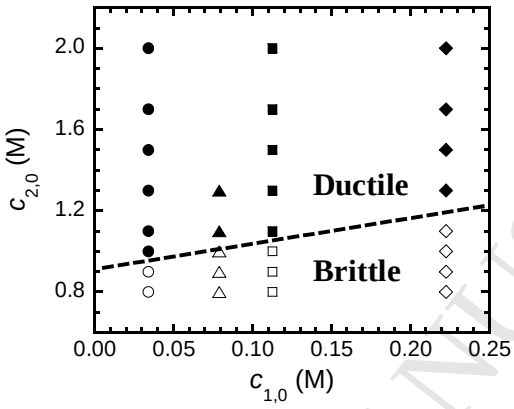

Figure 5: Composition-dependent brittle-ductile phase diagram for different sets of DN gels used in our work. $c_{1,0}$ and $c_{2,0}$ represent the true concentrations of the 1st and 2nd networks in the as-prepared DN gels, respectively. The circles (●), triangles (▲), squares (■) and diamond (♦) shapes indicate the samples DN (2/*y*), DN (3/*y*), DN (4/*y*), and DN (6/*y*), respectively; whereas the filled and open symbols indicate ductile and brittle samples respectively, identified from tensile and tearing test results of their *swollen* forms.

networks depends on the concentrations of the two components at which the IPN structure is formed, we adopt the 1st network and 2nd network concentrations, $c_{1,0}$ and $c_{2,0}$, respectively, of the as-prepared IPN samples. Here $c_{1,0}$ was estimated from the thicknesses of the PAMPS gels in their as-prepared and swollen states and $c_{2,0}$ was estimated as $c_{2,0}=c_{AAm}$, assuming 100% polymerization efficiency of the precursor monomers[26] (**Supporting Information**). **Figure 5** shows that the critical $c_{2,0}$ for transition only slightly increases with $c_{1,0}$. Based on the results of samples DN (2/*y*), DN (4/*y*), DN (6/*y*) shown in **Figures 2-4**, we synthesized additional samples

of DN (3/*y*) around the transition region and the results are also shown in **Figure 5**. The physical meaning of this exclusive phenomenon will be discussed later.

Mechanical Hysteresis Behavior. As has been revealed by the previous studies of our group, the DN gels are toughened by the internal fracture mechanism. This internal fracture of PAMPS remarkably increases the energy for crack growth and delocalizes the stress at the crack tip. As a result, the crack propagation in DN gels is retarded.[27,28] To relate the brittle-ductile transition to the structure change of the PAMPS network, we further characterized the internal fracture behavior of PAMPS by measuring the hysteresis of the repeated cyclic tensile elongation. The cyclic stress-strain (c-SS) curves of ductile DN (4/1.7) and brittle DN (4/1) gels are shown in **Figure 6**. The inset figure enlarges the c-SS curves for the brittle sample. For the ductile

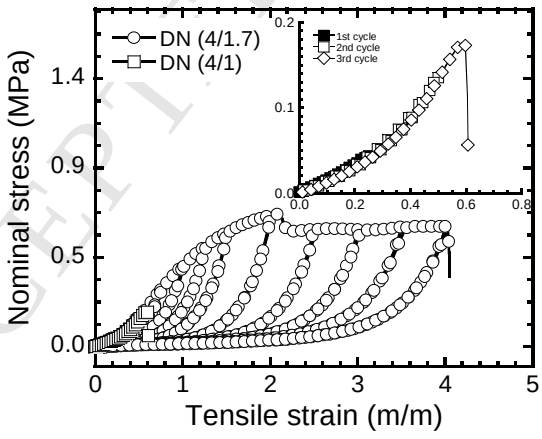

Figure 6: Comparative successive loading curves of brittle DN (4/1) and ductile DN (4/1.7) gels obtained from the cyclic tensile test after applying increasing amount of strain (until fracture). The inset figure provides an enlarged view of the curves of DN (4/1) including different loading cycles which overlap with each other showing almost no hysteresis till sample failure.

samples, they show very large amount of hysteresis (i.e. energy dissipation) above a certain strain, and the hysteresis increases with the applied strain until sample breakage. On the contrary, the brittle sample breaks at a very small strain and exhibits almost no hysteresis until breakage. Subsequently, we calculated the amount of dissipated energy from the area of the c-SS curves as a result of applying different amount of strain (**Figure 7a**) for the brittle (4/1), moderately tough (4/1.5) and the toughest (4/2) DN gels. DN (4/1.5) and DN (4/2) hydrogels initially exhibit very

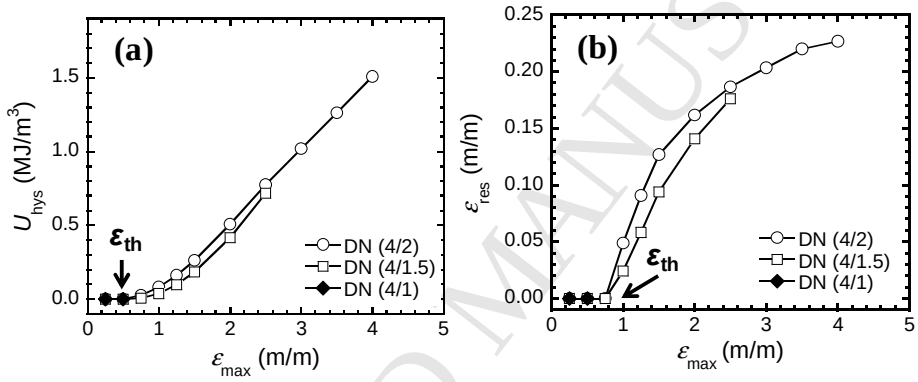

Figure 7: The trend of increasing **(a)** dissipated energy, U_{hys} and **(b)** residual strain, ε_{res} as function of the maximum applied strain, ε_{max} for brittle DN (4/1), moderately tough (4/1.5) and toughest (4/2) gels. The brittle gel fractures before reaching ε_{th}, without showing U_{hys} and ε_{res}.

little energy dissipation up to a certain strain (we assign it as the 'threshold strain for energy dissipation', ε_{th}) and then the energy dissipation increases linearly with increasing strain, in consistence with our recent works.[22] On the other hand, the brittle DN (4/1) shows almost no energy dissipation and fractures immediately once it reaches the ε_{th}. Apparently, ε_{th} is the point at which the internal fracture of the 1st network starts. For the brittle sample, this starting of the 1st network fracture leads to propagation of the micro crack and brings sudden global failure of both

the PAMPS and PAAm networks. On the other hand, for the ductile sample, the crack propagation of the 1st network is stopped by the PAAm network.

The internal structural change of materials usually brings about residual strain after deformation. We also investigated the residual strain for different cycles from the c-SS curves for the above-mentioned three compositions (**Figure 7b**). The brittle DN (4/1) sample that shows elastic behavior exhibits no residual strain until fracture at the ε_{th}. On the other hand, the ductile samples, DN (4/1.5) and DN (4/2), do exhibit residual strain above the threshold strain (ε_{th}), in consistence with the internal fracture of the 1st network. The residual strains, although very small in comparison with the large strains the samples experienced, go through a continuous increase with increasing applied strain. Considering the incompressible nature of gels (Poisson's ratio ν = 0.5), these residual strains should bring about a decrease in the cross sectional area of the sample, which can be attributed to the anisotropic fracture of the PAMPS network.[22]

From the above results, features of the brittle and the ductile DN gels can be distinguished as follows; the former are brittle, weak, and fracture before internal fracture of the 1st network whereas the latter are ductile, strong, and fracture after wide-range internal fracture of the 1st network. Therefore, brittle-ductile transition also can be defined by presence or absence of internal fracture.

The characteristic parameters for internal fracture, which are, stress and strain at the threshold point (where internal fracture starts to occur inside DN gels) and at the yielding point (where the 1st network starts to break into discontinuous fragments) are tabulated in *Table 2*. σ_{th} and ε_{th} are the stress and strain values at threshold, while σ_y and ε_y are the stress and strain at yield point, respectively.

Table 2. Fracture parameters for DN gels synthesized with different 1st network cross-linking density (x= 2, 3, 4 and 6 mol%), and different 2nd network concentration c_{AAm} (= y).

DN gel	σ_{th} **(MPa)**	ε_{th}	σ_y **(MPa)**	ε_y
DN (2/y)	0.08~0.1	1.0	0.1~0.2	1.9
DN (3/y)	0.2~0.3	1.1	0.2~0.3	1.8
DN (4/y)	0.4~0.6	0.9	0.6~0.8	1.8
DN (6/y)	0.9~1.1	0.7	1.2~1.5	1.6

*As the stress values vary slightly depending on the 2nd network concentrations, we showed the range of original values. The strain values are almost independent of c_{AAm}, thus the average values are shown.

Structural Parameters Governing the Transition. Now, the question is what is the key structural parameter that governs the occurrence of effective internal fracture, and therefore the brittle-ductile transition? To answer this question, we investigated the tensile behaviors of individual single network PAMPS gels in swollen state and PAAm gels in as-prepared state, with the same formulation as that of as-prepared DN gels. As shown in **Figure 8**, PAMPS gels are rigid and brittle; thus they fracture at very small strains (nominal fracture strain, ε_f <0.35). On the other hand, PAAm gels are soft and ductile, showing large fracture strains (ε_f =15-35). The mechanical parameters for swollen single PAMPS and as-prepared single PAAm gels, are tabulated in *Supporting Information Tables S1* and *S2*, respectively, where E^s, σ_f^s and ε_f^s are Young's modulus, fracture stress, and fracture strain of these single network gels, respectively. The polymer strands number density, v_e^s, estimated from the Young's modulus of the gels

(**Supporting Information**), and the chain stiffness of swollen PAMPS gels, e_n ($e_n = \frac{E_1^s}{3\nu_{e,1}^s RT}$) in relative to the Gaussian chains, is also shown in those tables.

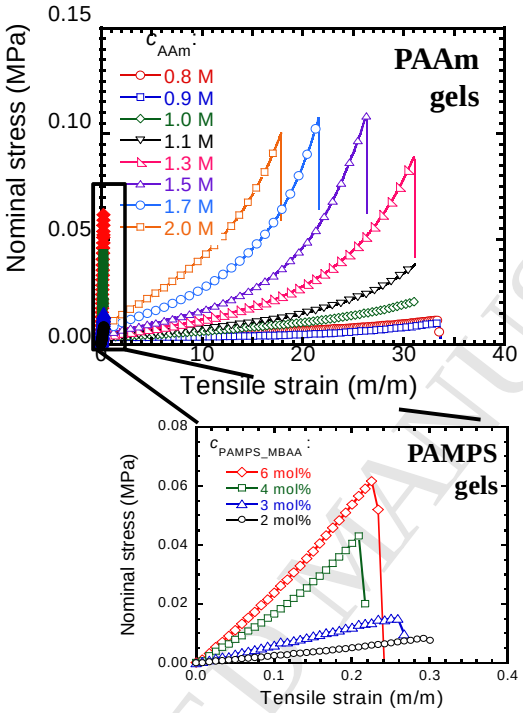

Figure 8: The tensile SS curves of sole PAMPS and PAAm gels having the same concentrations as in their corresponding DN gels. Only a portion of data is shown for a clearer view. Tensile SS curves of sole PAMPS gels are magnified in to a separate figure in the bottom for better visibility.

It should be mentioned that $\nu_{e,2}^s$ of PAAm gels includes the polymer strands from chemical cross-linking $\nu_{e,2}^c$ and trapped self-entanglement between 2nd network polymer strands $\nu_{e,2}^{self}$. That is,

$$\nu_{e,2}^s = \nu_{e,2}^c + \nu_{e,2}^{self} \quad (4)$$

Since we used extremely low amount of chemical cross-linker (1 mole of cross-linker for every 5000 moles of monomer) for 2nd network preparation, the physical entanglement term $\nu_{e,2}^{self}$ is predominant in $\nu_{e,2}^{s}$.

Comparing the results in *Table 2* and *Table S1*, we observe that the fracture stress of single PAMPS $\sigma_{f,1}^{s}$ is much lower than the threshold stress σ_{th} of DN gels, that is, $\sigma_{f,1}^{s} \ll \sigma_{th}$. This indicates that when fracture occurs in single PAMPS gel, it quickly turns into a global failure. On the other hand, crack propagation, or wide-scale internal fracture of PAMPS is prevented by the 2nd network in DN gels, even at a 2nd network concentration below the brittle-ductile transition.

As DN gels consist of two interpenetrated networks, the B-D transition is governed by the mechanical balance of the two networks.[3,14] The load transfer between the networks is through the trapped, topological entanglement between the two networks. Assuming that the two networks are homogeneous, the strength of the 1st and 2nd networks in DN gels can be expressed as follows,

$$\sigma_{f,1} = (\nu_{e,1} N_A)^{2/3} f_1 \quad (5)$$

$$\sigma_{f,2} = (\nu_{e,2} N_A)^{2/3} f_2 \quad (6)$$

where ν_e is the polymer strands number density, σ_f and f are the fracture stress of the corresponding network and the fracture force of single polymer strand, respectively. So, the mechanical balance between the two networks is determined by the condition $\sigma_{f,2}/\sigma_{f,1} \gg 1$. As both the first and the second network strands consist of C-C bonds, they have the same bond breaking strength, that is, $f_1 = f_2$ in the present case. So the mechanical balance of the two

networks should be essentially controlled by the chain density balance, $(\nu_{e,2}/\nu_{e,1})^{2/3} \gg 1$. To confirm this assumption, we need to estimate $\nu_{e,1}$ and $\nu_{e,2}$ in the as-prepared DN gels.

Since the 1st network is much more rigid than the 2nd network, and the modulus of the DN gels is approximately equal to the sole swollen PAMPS gels, we assume that chain density of PAMPS in DN gel, $\nu_{e,1}$ is equal to that of the sole PAMPS gel in swollen state, $\nu_{e,1}^{s}$, i.e.,

$$\nu_{e,1} = \nu_{e,1}^{s} \quad (7)$$

On the other hand, $\nu_{e,2}$ of the second soft network in DN gels should come from two contributions: the contribution from the sole PAAm network $\nu_{e,2}^{s}$ and the contribution from entanglement of second network to the first network ν_{e}^{inter}.

$$\nu_{e,2} = \nu_{e,2}^{s} + \nu_{e}^{inter} \quad (8)$$

The contribution of internetwork entanglement ν_{e}^{inter} to $\nu_{e,2}$ is prominent, as can be observed in **Figure 3c**. We found that ε_f of DN gels decreases with increasing first network cross-linker density *x*, indicating that the enhanced entanglement of the second network with the first network decreases the extensibility of PAAm chains.

Assuming that the polymerization of AAm monomers in the presence of PAMPS network is the same as that of sole PAAm gel,[21] $\nu_{e,2}^{s}$ is equal to that of the single PAAm gels in the as-prepared state. Then, the question is how to estimate ν_{e}^{inter}. Let us consider two kinds of cubic lattices with a number density of m_1^3 and m_2^3 in three-dimensional space, respectively. Now, if we overlap these two lattices such that their edges are in complete matching, then the cross-over of the lattice bonds splits the lattices into even smaller lattices. The total lattice

number density now becomes $m^3 = (m_1+m_2)^3$. We can think these two lattices as the two networks of DN gels, and the cross-over points of the lattices as the internetwork entanglement points. So the polymer strand densities of the individual 1st and 2nd networks $\nu_{e,1}^s$ and $\nu_{e,2}^s$ can be related to m_1 and m_2 as $\nu_{e,1}^s \sim {m_1}^3$ and $\nu_{e,2}^s \sim {m_2}^3$, and the total polymer strand density ν_e^{total} of the DN gels is then given by

$$\nu_e^{total} = ({\nu_{e,1}^s}^{1/3} + {\nu_{e,2}^s}^{1/3})^3 \qquad (9)$$

Equation 9 can be expanded as,

$$\nu_e^{total} = \nu_{e,1}^s + \nu_{e,2}^s + 3\,{\nu_{e,1}^s}^{1/3}\,{\nu_{e,2}^s}^{1/3}({\nu_{e,1}^s}^{1/3} + {\nu_{e,2}^s}^{1/3}) \qquad (10)$$

The 1st and 2nd terms of the above equation are the polymer strand densities of the sole 1st and 2nd networks separately, while the 3rd term represents the strand densities owing to the internetwork entanglement between two networks. That is,

$$\nu_e^{inter} = 3\,{\nu_{e,1}^s}^{1/3}\,{\nu_{e,2}^s}^{1/3}({\nu_{e,1}^s}^{1/3} + {\nu_{e,2}^s}^{1/3}) \qquad (11)$$

Thus, the total polymer strand densities of the 2nd network inside DN gel including the internetwork entanglement is expressed as follows,

$$\nu_{e,2} = \nu_{e,2}^s + 3\,{\nu_{e,1}^s}^{1/3}\,{\nu_{e,2}^s}^{1/3}({\nu_{e,1}^s}^{1/3} + {\nu_{e,2}^s}^{1/3}) \qquad (12)$$

It is easy to find that the 2nd term in Equation 12 is dominant for $\frac{\nu_{e,2}^s}{\nu_{e,1}^s} < 55$. This condition is always satisfied within the experimentally accessible range, as shown by **Figure 9a**. This indicates that the 2nd network strands density is always dominated by the internetwork

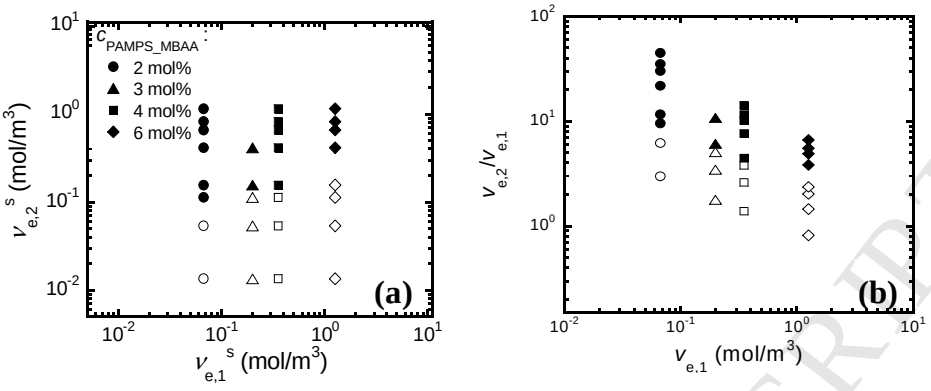

Figure 9: Brittle-ductile phase diagrams in polymer strand density space. **(a)** $\nu_{e,2}^{s}$ vs. $\nu_{e,1}^{s}$, without considering the internetwork entanglement; **(b)** $\nu_{e,2}/\nu_{e,1}$ vs. $\nu_{e,1}$, after including the inter-network entanglement term for the second network.

entanglement effect. **Figure 9b** shows the ratio of the polymer strand density, $\nu_{e,2}/\nu_{e,1}$ thus calculated for various DN gels. Using Eqs. 5 and 6, the fracture stress ratio is also calculated by the following equation,

$$\sigma_{f,2}/\sigma_{f,1} = (\nu_{e,2}/\nu_{e,1})^{2/3} \quad (13)$$

The $\nu_{e,2}$, $\nu_{e,2}/\nu_{e,1}$, and $\sigma_{f,2}/\sigma_{f,1}$ values around the B-D transition region (nearest ductile point around transition) are shown in *Table 3*. The result indicates that the brittle-ductile transition of DN gels occurs at a critical polymer strand densities ratio $(\nu_{e,2}/\nu_{e,1})_{B-D} = k$ of 3.8-9.5, which is equivalent to a strength ratio of $(\sigma_{f,2}/\sigma_{f,1})_{B-D} = k^{2/3}$ of 2.5-4.5. When $(\nu_{e,2}/\nu_{e,1}) > k$, DN gels become ductile and tough. Conversely, when $(\nu_{e,2}/\nu_{e,1}) < k$, the DN gels are weak and brittle.

The stiffness of each stretched 1st network strand is much higher than that of the 2nd network strand which is in random coil state, as revealed by e_n, the chain stiffness relative to a Gaussian chain, in **Figure 3**. So at small deformation, the stress ratio of the two networks $\sigma_2/\sigma_1 = \nu_{e,2}/\nu_{e,1}e_n$ is much smaller than one. Even at the yielding strain ε_y, the stress sustained by the 2nd network is still negligible compared to the 1st network. This can be easily confirmed by comparing the yield stress σ_y with the stress of the 2nd network σ_2 at yielding point. At ε_y, the 2nd network is still in the linear elastic deformation, and noting that σ_y was measured from swollen DN gels, so we measured σ_2 using $\sigma_2 = 3\nu_{e,2}(t_{DN}^0/t_{DN})^3 RT\varepsilon_y$. Here $(t_{DN}^0/t_{DN})^3$ stands for the volume change of 1st network from the as-prepared state to swollen state. We found that $\sigma_{2,swelling} << \sigma_y$ as shown in *Table 3*. This indicates that in order to sustain the load after the breaking of the 1st network, the surrounding 2nd network should be in highly stretched state so that strain hardening occurs.

Table 3. Structure and stress parameters of DN gels around the B-D transition region.

	As-prepared DN			***Swollen DN***	
c_{PAMPS_MBAA} **(mol%)**	$(\nu_{e,2})_{B\text{-}D}$ **(mol/m^3)**	$(\nu_{e,2}/\nu_{e,1})_{B\text{-}D}$	$(\sigma_{f,2}/\sigma_{f,1})_{B\text{-}D}$	$\sigma_{f,1}/\sigma_y$	$\sigma_{2,swelling}/\sigma_y$ (At $\varepsilon = \varepsilon_y$)
2	0.636	9.529	4.495	11.903	0.039
3	1.217	6.086	3.333	15.939	0.041
4	1.575	4.476	2.716	10.010	0.022
6	4.823	3.834	2.450	11.779	0.024

As shown in **Figure 2** and *Table 2*, the yielding stress σ_y increases with the 1st network concentration but also shows a slight dependence on the second network concentration. Here, we discuss the relation between σ_y and the fracture stress of the 1st network $\sigma_{f,1}$. The latter is estimated from Eq. 5, based on the structure at small strain. The ratio $\sigma_{f,1}/\sigma_y$ is shown in *Table 3*. In the calculation, the 1st network strand density in the swollen DN gels was used and the force to break the C-C bond was used as f =2 nN.[29] The $\sigma_{f,1}$ is about 11-16 times higher than σ_y experimentally observed, regardless the crosslinker density of the 1st network. Apparently, this large difference should, first of all, come from the large inhomogeneity of the first network, as short strands start to break far below the yielding point in the real DN gels while homogenous structure was assumed to calculate $\sigma_{f,1}$. However, as revealed in our previous works, only about 1% of the short strands of the 1st network are unloaded before the yielding strain ε_y.[22] So the large difference of $\sigma_{f,1}$ and σ_y could not be explained by the inhomogeneity effect.

Two-Spring Model for Brittle-Ductile Transition. The previous experiments and analyses clearly show that the essence of the brittle-ductile transition is the mechanical balance of the two networks, whereupon the internetwork entanglement play important role. Based on this result, we try to illustrate this brittle-ductile transition in double network gels adopting a two-spring model as shown in **Figure 10**. The blue and red springs signify the state of the 1st and 2nd network strands in DN gel, respectively. For both brittle and ductile gels, the stiff and short PAMPS strands that are in highly extended state fracture first, starting from the threshold strain, ε_{th}. Once this happens, the applied force is transferred to the soft and long PAAm strands that are in coiled state through internetwork entanglement, making them locally stretched. Now, if

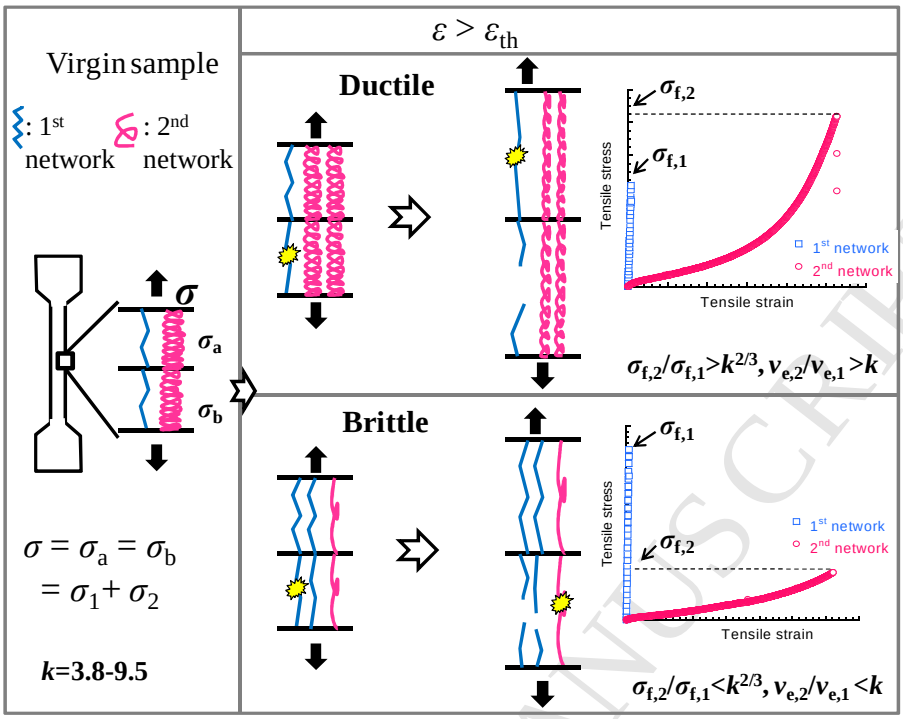

Figure 10: Two springs model showing a molecular picture of the brittle-ductile transition of DN gels. The mechanical force balance between the 1st and 2nd network governs the transition. The force balance is related to the polymer strand density ratio, in which the internetwork entanglement dominates the 2nd network strand density.

$\frac{\nu_{e,2}}{\nu_{e,1}} > k(= 3.8 - 9.5)$, corresponding to a fracture stress ratio $\sigma_{f,2}/\sigma_{f,1} = k^{2/3}$, these PAAm strands can sustain the force transferred by large deformation to level that the strain-hardening occurs. As the two networks are strongly entangled with each other, the stretched PAAm strands further transfer force to PAMPS strands and induce their fracture, which leads to wide-range internal fracture of PAMPS, *i.e.* high toughness of DN gels. Oppositely, if $\frac{\nu_{e,2}}{\nu_{e,1}} < k$, these PAAm strands cannot sustain the stress and fracture right after the fracture of PAMPS strands. As a result, global sample failure occurs without large energy dissipation.

IV. Conclusions

The composition-dependent brittle-ductile transition of DN gels is determined by the mechanical balance of the two networks, in which the effective polymer strand density ratio of the two networks, $\nu_{e,2}/\nu_{e,1}$, serves as the key parameter. The $\nu_{e,2}$ of the second network in DN gels is dominated by internetwork entanglement. When the ductile second network has much more strand density than the brittle first network ($\nu_{e,2}/\nu_{e,1}>k$ =3.8-9.5), the DN gels become tough. Conversely, when $\nu_{e,2}/\nu_{e,1}< k$, the DN gels become brittle. As the brittle network is comprised of short and extended chains, it always ruptures first, by which the stress is transferred to the ductile network. In the case of $\nu_{e,2}/\nu_{e,1} > k$, the propagation of the micro-crack in the brittle network is stopped by the ductile network, and the latter transfer the stress to a wide region to cause further internal damage of the brittle network. As a result, the brittle network dissipates large amount of energy working as sacrificial bonds and the toughness of the gels is abruptly enhanced. On the other hand, in the case of $\nu_{e,2}/\nu_{e,1}< k$, the ductile network cannot sustain the force transferred from the brittle network, and it ruptures simultaneously. As a result, the crack propagates catastrophically which leads to an immediate grand failure of the sample to show brittleness. This immediate fracture of PAAm network just after that of PAMPS prevents the internal fracture of the 1st network, thus leads to negligible energy dissipation by brittle samples. Accordingly, a mechanical definition of the DN hydrogels is different from the IPN hydrogels in the sense that DN hydrogels have internal fracture before failure. The criteria $\nu_{e,2}/\nu_{e,1}> k$ for obtaining tough DN gels is universal and should be used as the key parameter to design tough materials based on the double network concept.

Acknowledgement

This work was supported by a Grant-in-Aid for Scientific Research (S) (No. 124225006) from Japan Society for the Promotion of Science (JSPS).

References

1. Gong, J. P.; Katsuyama, Y.; Kurokawa, T.; Osada, Y. *Adv. Mater.* **2003**, *15*, 1155.
2. Kawauchi, Y.; Tanaka, Y.; Furukawa, H.; Kurokawa, T.; Nakajima, T.; Osada Y.; Gong, J. P. *J. Phys. Conf. Ser.* **2009**, *184*, 012016.
3. Tanaka, Y.; Kuwabara, R.; Na, Y. –H.; Kurokawa, T.; Gong, J. P.; Osada, Y. *J. Phys. Chem. B.* **2005**, *109*, 11559.
4. Nakajima, T.; Furukawa, H.; Tanaka, Y.; Kurokawa, T.; Osada Y.; Gong, J. P. *Macromolecules* **2009**, *42*, 2184.
5. Hu, J.; Kurokawa, T.; Hiwatashi, K.; Nakajima, T.; Wu, Z. L.; Liang S.; Gong, J. P. *Macromolecules* **2012**, *45*, 5218.
6. Nakajima, T.; Sato, H.; Zhao, Y.; Kawahara, S.; Kurokawa, T.; Sugahara, K. Gong, J. P. *Adv. Funct. Mater.* **2012**, *22*, 4426.
7. Suekama, T. C.; Hu, J.; Kurokawa, T.; Gong, J. P., Gehrke, S. H. *ACS Macro Lett.* **2013**, *2*, 137.
8. Nakajima, T.; Fukuda, Y.; Kurokawa, T.; Sakai, T.; Chung, U.; Gong, J. P. *ACS Macro Lett*. **2013**, *2*, 518.
9. Haiyan, Y.; Akasaki, T.; Sun, T. L.; Nakajima, T.; Kurokawa, T.; Nonoyama, T.; Taira, T.; Saruwatari, Y.; Gong, J. P. *J. Mater. Chem. B* **2013**, *1*, 3685.
10. Na, Y. –H.; Tanaka, Y.; Kawauchi, Y.; Furukawa, H.; Sumiyoshi, T.; Gong, J. P.; Osada, Y. *Macromolecules* **2006**, *39*, 4641.
11. Webber, R.; Creton, C.; Brown, H. R.; Gong, J. P. *Macromolecules* **2007**, *40*, 2917.
12. Brown, H. R. *Macromolecules* **2007**, *40*, 3815.
13. Tanaka, Y. *Europhys. Lett*. **2007**, *78*, 56005.

14. Wang, X; Hong, W. *Soft Matter* **2011**, *7*, 8576.

15. Na, Y. –H.; Kurokawa, T.; Katsuyama, Y.; Tsukeshiba, H.; Gong, J. P.; Osada, Y.; Okabe, S.; Karino, T.; Shibayama, M. *Macromolecules* **2004**, *37*, 5370.

16. Tominaga, T.; Tirumala, V. R.; Lin, E. K.; Gong, J. P.; Wu, W. –L. *J. Phys. Chem. B* **2007**, *112*, 3903.

17. Rivlin, R. S.;Thomas, A. G. *J. Polym. Sci.***1953**, *10*, 291.

18. Greensmith, H. W.;Thomas, A. G. *J. Polym. Sci*.**1955**, *18***,** 189.

19. Furukawa, H.; Kuwabara, R.; Tanaka, Y.; Kurokawa, T.; Na, Y. –H.; Osada, Y.; Gong, J. P. *Macromolecules* **2008**, *41*, 7173.

20. Hertzberg, R. In *Deformation and Fracture Mechanics of Engineering Materials*, John Wiley and Sons: New York, 1996; p 757.

21. Tsukeshiba, H.; Huang, M.; Na, Y. –H.; Kurokawa, T.; Gong, J. P.; Osada, Y. *J. Phys. Chem. B*. **2005**, *109*, 11559.

22. Nakajima, T.; Kurokawa, T.; Ahmed, S.; Wu, W. –L.; Gong, J. P. *Soft Matter* **2013**, *9*, 1955.

23. Lin, W. –C.; Fan, W.; Marcellan, A.; Hourdet, D.; Costantino, C. *Macromolecules* **2010**, *43*, 2554.

24. Evans, A. G. In *Fracture mechanics of ceramics*, Plenum, New York, 1974; Vol. 1, p 17.

25. Zarzycki, J. *J. Non-Cryst. Solids* **1988**, *100*, 359.

26. Kii, A.; Xu, J.; Gong, J. P.; Osada, Y.; Zhang, X. *J. Phys. Chem. B* **2001**, *105*, 4565.

27. Tanaka, Y.; Kawauchi, Y.; Kurokawa, T.; Furukawa, H.; Okajima, T.; Gong, J. P. *Macromol. Rapid Commun*. **2008**, *29*, 1514.

28. Yu, Q. M.; Tanaka, Y.; Furukawa, H.; Kurokawa, T.; Gong, J. P. *Macromolecules* **2009**,

42, 3852.

29. Grandbois, M.; Beyer, M.; Rief, M.; Clausen-Schaumann, H.; Gaub, H. E. *Science* **1999**, *283*, 1727.

For Table of Contents (TOC) use only

Brittle-Ductile Transition of Double Network Hydrogels: Mechanical Balance of Two Networks as the Key Factor

Saika Ahmed, Tasuku Nakajima, Takayuki Kurokawa, Md. Anamul Haque, and Jian Ping Gong

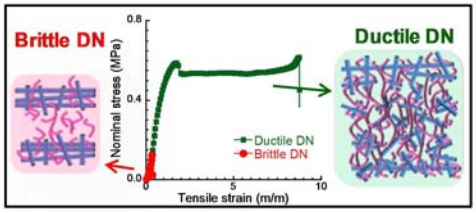

Supporting Information

Brittle-Ductile Transition of Double Network Hydrogels: Mechanical Balance of Two Networks as the Key Factor

*Saika Ahmed, Tasuku Nakajima, Takayuki Kurokawa, Md. Anamul Haque, Jian Ping Gong**

Concentration of the Two Networks:

The as-prepared PAMPS gels substantially swelled in water and the thickness of the swollen PAMPS gels increased with decreasing c_{1_MBAA}. The thickness of PAMPS gels in different AAm monomer concentrations remained the same as that in water. After the second polymerization of AAm, the as-prepared DN gels further swelled in water and the gels thickness increased with increasing AAm concentration c_{AAm}. Since DN gels show isotropic swelling, we calculated the concentrations of PAMPS and PAAm in the as-prepared DN gels, which are indicated as $c_{1,0}$ and $c_{2,0}$ respectively, and in the swollen DN gels, which are indicated as c_1 and c_2 respectively, from the thickness changes of the samples. Assuming 100% conversion of the monomers in polymerization for both networks,[1] we have

$$c_{1,0} = c_{\mathrm{AMPS}} \left(\frac{t^0_{\mathrm{PAMPS}}}{t_{\mathrm{PAMPS}}}\right)^3 \qquad \text{(S1)}$$

$$c_{2,0} = c_{\mathrm{AAm}} \quad \text{(S2)}$$

$$c_1 = c_{\mathrm{AMPS}} \left(\frac{t^0_{\mathrm{PAMPS}}}{t_{\mathrm{DN}}}\right)^3 \quad \text{(S3)}$$

$$c_2 = c_{\mathrm{AAm}} \left(\frac{t^0_{\mathrm{DN}}}{t_{\mathrm{DN}}}\right)^3 \quad \text{(S4)}$$

Where, c_{AMPS} is the concentration of AMPS in the precursor solution (fixed as 1 M) of the PAMPS gels, $t_{\mathrm{PAMPS}}{}^0$ is the thickness of the as-prepared PAMPS gels (fixed as 1 mm), t_{PAMPS} is the thickness of swollen PAMPS gels in water/AAm precursor solution, c_{AAm} (M) is the AAm concentration in the precursor solution for preparing DN gels, $t_{\mathrm{DN}}{}^0 (= t_{\mathrm{PAMPS}})$ and t_{DN} are the thicknesses of the as-prepared and swollen DN gels, respectively.

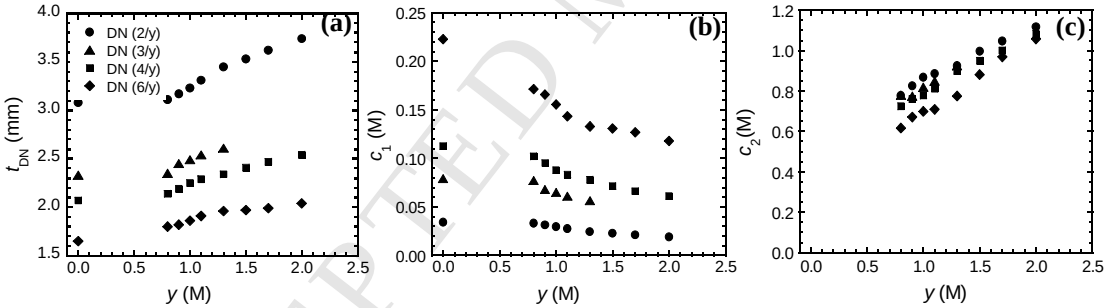

Figure S1: (a) Thickness of swollen DN gels, t_{DN}; for different in feed AAm concentrations, c_{AAm} (y) at various c_{1_MBAA} (x), and the true concentrations of **(b)** PAMPS, c_1 and **(c)** PAAm, c_2 in these DN gels. The circles (●), triangles (▲), squares (■) and diamonds (♦) indicate the samples with 2, 3, 4 and 6 mol% of c_{1_MBAA} respectively.

The final thickness of the swollen DN gels (*t*-DN) of **Table 1** is shown in **Figure S1a**. The true concentrations of the individual networks in different samples DN (*x*/*y*), obtained from their

swollen thicknesses, are summarized in **Figures S1b** and **S1c** for c_1 and c_2, respectively, where *x* and *y* refer to the PAMPS gel cross-linker density, c_{1_MBAA} and second network AAm monomer concentration in feed, c_{AAm}, respectively.

As the PAMPS single network already reaches its equilibrium swelling state in AAm precursor solution and this equilibrium swelling in AAm solution is the same as that in pure water, the further swelling of the DN gels in water after synthesis is due to the osmotic pressure of PAAm. That is, the equilibrium swelling of DN gels in water is determined by the balance between the osmotic pressure of loosely crosslinked PAAm network that is entrapped inside the densely crosslinked PAMPS network, and the elasticity of the PAMPS polymers. This explanation is confirmed by the fact that the DN gels show the same swelling in NaCl solution as that in water.[2]

Structure Parameters in Single Network Gels:

The $\nu_{e,1}^{s}$ and $\nu_{e,2}^{s}$, which are number densities of elastically effective polymer strands of swollen 1st network and as-prepared 2nd network, can be estimated from the Young's moduli *E* of the individual gels according to the rubber elasticity theory. For elastic strands in Gaussian conformation,

$$E = 3\nu_e RT \quad \text{(S5)}$$

where *R* is gas constant and *T* is temperature. As the polymer strands of swollen PAMPS gel are in highly extended conformation, we could not apply Eq. S5 directly to estimate $\nu_{e,1}^{s}$. Instead, we first estimated the strand density of as-prepared PAMPS gels and then, we estimated $\nu_{e,1}^{s}$ using the following Equation S6.

$$\nu_{e,1}^{s} = \frac{E_0}{3RT}\left(\frac{t_{PAMPS}^{0}}{t_{PAMPS}}\right)^3 \quad \text{(S6)}$$

where, E_0 is the Young's modulus of the as-prepared PAMPS gels, $t_{PAMPS}{}^{0}$ and t_{PAMPS} are the thicknesses of as-prepared and equilibrium swollen PAMPS gels, respectively (**Table S1**). The chain stiffness of swollen PAMPS gels, e_n, at different c_{PAMPS_MBAA} is measured by the following equation and also shown in Table S1.

$$e_n = \frac{E_1^s}{3\nu_{e,1}^{s} RT} \quad \text{(S7)}$$

where $E_1{}^{s}$ is the Young's modulus of swollen PAMPS gels.

Since the polymer strands in the neutral PAAm gel are in Gaussian conformation, we simply estimated $\nu_{e,2}^{s}$ from the as-prepared PAAm gels by Equation S5 (values in ***Table S2***).

Table S1. Structural and mechanical parameters for swollen single network PAMPS gels prepared at different c_{PAMPS_MBAA}.

c_{PAMPS_MBAA} (mol%)	E_0 (kPa)	E_1^s (kPa)	t_{PAMPS} (mm)	$\nu_{e,1}^s$ (mol/m^3)	$e_{n,1}$	$\varepsilon_{f,1}^s$	$\sigma_{f,1}^s$ (MPa)
2	14.5	25.1	3.08	0.067	50.38	0.32	0.006
3	18.8	63.2	2.33	0.200	43.06	0.28	0.019
4	23.2	84.1	2.07	0.352	32.12	0.23	0.047
6	42.0	120.5	1.65	1.258	12.84	0.23	0.062

Note: t_{PAMPS}^0= 1mm. E_0 is the Young's modulus at as-prepared state, $\varepsilon_{f,1}^s$ and $\sigma_{f,1}^s$ are the fracture strain and stress of swollen sole PAMPS gels, respectively.

*Parameter values shown are average of 4 samples for each composition.

Table S2. Structure and mechanical parameters for single network PAAm gels prepared at different c_{AAm}.

c_{AAm} (M)	E_0 (kPa)	$\nu_{e,2}^{s}$ (mol/m^3)	$\varepsilon_{f,2}{}^{s}$	$\sigma_{f,2}{}^{s}$ (MPa)
0.8	0.1	0.013	37.22	0.009
0.9	0.4	0.054	33.10	0.008
1.0	0.8	0.113	31.65	0.021
1.1	1.2	0.156	30.61	0.028
1.3	3.1	0.415	28.78	0.080
1.5	4.9	0.662	25.26	0.087
1.7	6.1	0.823	22.45	0.106
2.0	8.5	1.148	20.88	0.165

Note: E_0 is the Young's modulus at as-prepared state, $\varepsilon_{f,2}{}^{s}$ and $\sigma_{f,2}{}^{s}$ are the fracture strain and stress of as-prepared sole PAAm gels, respectively.

*Parameter values shown are average of 4 samples for each composition.

References

1. Kii, A.; Xu, J.; Gong, J. P.; Osada, Y.; Zhang, X. *J. Phys. Chem. B* **2001**, *105*, 4565.

2. Haiyan, Y.; Akasaki, T.; Sun, T. L.; Nakajima, T.; Kurokawa, T.: Nonoyama, T.; Taira, T.; Saruwatari, Y.; Gong, J. P. *J. Mater. Chem. B* **2013**, *1*, 3685.